THE ASTROPHYSICAL JOURNAL, 460:634–643, 1996 April 1

COMPACT SYMMETRIC OBJECTS AND THE EVOLUTION OF POWERFUL EXTRAGALACTIC RADIO SOURCES

A. C. S. READHEAD, G. B. TAYLOR, AND T. J. PEARSON
Radio Astronomy, California Institute of Technology, 105–24, Pasadena, CA 91125

AND

P. N. WILKINSON
University of Manchester, Nuffield Radio Astronomy Laboratories,
Jodrell Bank, Macclesfield, Cheshire SK11 9DL, UK
Received 1995 May 25; accepted 1995 October 3

ABSTRACT

Multifrequency radio observations of the compact symmetric objects 0108+388, 0710+439 and 2352+495, and high-resolution VLA observations of the primary hot spot in Cygnus A, are used to investigate the dependence on external density of the size, pressure, advance speed, and flux density of the hot spots in powerful extragalactic radio sources. The relationships derived are applied over the whole range of scales observed in these objects.

These relationships lead directly to a unifying evolutionary model for powerful radio sources, in which compact symmetric objects evolve first into compact steep spectrum doubles, and then into large Fanaroff-Riley type II objects. We propose that this is the primary evolutionary track for powerful extragalactic radio sources. The observations strongly suggest that these objects evolve substantially in luminosity, with little variation in expansion speed between 10 pc and 200 kpc.

Subject headings: galaxies: active — galaxies: compact — galaxies: jets — radio continuum: galaxies

1. INTRODUCTION

The evolution of powerful extragalactic radio sources has been a fundamental problem in the study of active galaxies since Jennison & Das Gupta (1954) showed that the dominant radio emission in Cygnus A arose from two well-separated components, and Baade & Minkowski (1954) identified this radio source with an elliptical galaxy at a redshift of 0.057. Early attempts to model the evolution of these objects assumed that the radio components were ejected in a single burst of activity (De Young & Axford 1967; Ryle & Longair 1967), but these were superseded by theoretical models which assumed that the radio components were continuously supplied with energy from the center of activity (Rees 1971; Blandford & Rees 1974; Scheuer 1974), and, observationally, by the landmark paper of Hargrave & Ryle (1974), in which it was demonstrated that the radiation lifetime of the electrons in the hot spots of Cygnus A is significantly shorter than the light-travel time from the nucleus to the hot spots, making it clear that the observations demanded continuous energy supply from the central engine to the outer lobes.

Over the last 20 years "jets," along which the energy and momentum are supplied to the outer lobes, have been discovered in many active galaxies (e.g., Turland 1975; Waggett, Warner, & Baldwin 1977; Readhead, Cohen, & Blandford 1978; Perley, Dreher, & Cowan 1984; Bridle & Perley 1984). The question of the evolution of powerful extragalactic radio sources has therefore focused on the physics of jets. This has led to increasingly sophisticated hydrodynamic simulations of jets (Norman et al. 1982; Norman, Winkler, & Smarr 1983, 1984; Wilson & Scheuer 1983; Smarr, Norman, & Winkler 1984; Leahy & Williams 1984; Clark, Norman, & Burns 1986; Lind et al. 1989; Kossl et al. 1990a, b, c; Clarke 1993). A recent review of the status of simulations has been given by Norman (1993). In spite of the impressive progress in simulations, they have not yet converged on a standard model for powerful extragalactic radio souces. The requirements for fully three-dimensional simulations of a relativistic magnetized jet are daunting even by the standards of large parallel computers, although the problem is now tractable (Clarke 1993). But we do not yet know, for example, whether the magnetic field plays an important role in confining the hot spots. Such questions must be answered before we can use simulations to determine the evolution of these objects.

The ultimate aim of studies of the evolution of powerful extragalactic radio sources is to establish the relationships between the jet power or thrust, the luminosity, the size of the emission regions, the overall size, and the conditions in the external medium. An immediate objective is to determine the evolutionary tracks in the luminosity-size, or *P-D*, diagram (Baldwin 1982)—although other variables, such as jet power or thrust, might be more suitable for this purpose. One might hope to find the primary evolutionary paths by observation, just as was done for stellar evolution, and hope that this might provide a deeper physical insight into active galaxies. However, in spite of the wealth of observational data on both small- and large-scale structures of powerful extragalactic radio sources, it has not thus far proved possible to establish their evolution. Attempts to unify different classes of powerful extragalactic radio sources in a single evolutionary sequence (Readhead & Hewish 1976; Carvalho 1985; Hodges & Mutel 1987) have lacked a physical basis and remain unproved.

In this paper we present results of observations of compact symmetric objects (CSOs), which enable us to determine empirically the relationship between the most basic physical parameters of a relativistic jet and the density of the external medium. We show that CSOs provide a useful new laboratory for the study of the physics of rela-

tivistic jets, and that the empirical relationships derived provide a physical foundation for the study of the evolution of powerful extragalactic radio sources in the *P-D* diagram.

This paper is the third in a series of papers on CSOs based on the results of two dual-frequency VLBI surveys of complete samples selected at 5 GHz. In Paper I (Wilkinson et al. 1994) we showed that relativistic beaming in the outer lobes of these objects is either weak or absent. In Paper II (Readhead et al. 1995) we presented the statistics of the objects in different classes in the Pearson-Readhead (PR) sample and the first Caltech–Jodrell Bank (CJ1) sample (Pearson & Readhead 1988; Polatidis et al. 1995; Thakkar et al. 1995; Xu et al. 1995). In Paper II we used multi-frequency VLBI observations of 2352+495 to determine the physical properties of the radio emission regions of this object, and discussed in detail the physics of the two oppositely directed jets. This discussion lays the foundation for the present paper. We have carried out a similar analysis to that described in Paper II for the CSOs 0108+388 and 0710+439. The assumptions that we have used in determining the physical properties of the radio emission regions are given in Paper II.

We assume throughout this paper an Einstein–de Sitter universe with a Hubble constant $H_0 = 100\ h$ km s^{-1} Mpc^{-1}.

2. EVOLUTIONARY MODELS

2.1. *Theoretical and Empirical Approaches to Evolution*

The evolution of powerful extragalactic radio sources depends upon a number of areas of astrophysics which are poorly understood. These include the central engine, fueling, and jet interactions with the external medium. Significant progress has been made in theoretical models of the central engine (e.g., Blandford 1989, 1993) and in simulations of relativistic jets (Norman 1993). However, few observations are available to test models of the central engine, although recent X-ray observations are now changing this situation (Fabian 1995).

No simulations have addressed the question of the *evolution* of powerful extragalactic radio sources. Past attempts to describe their evolution have assumed a theoretical model (De Young & Axford 1967; Ryle & Longair 1967; Scheuer 1974; Carvalho 1985; Fanti et al. 1995), and then derived the expected evolutionary behavior. An alternative approach, opened up by large VLBI surveys, is to derive empirical relationships from the observations, and to use these relationships to predict results which test theory and/or simulations. We suggest three main lines of attack in determining the empirical relationships which describe the evolution of these objects: (1) comparisons of the radio emission regions in powerful extragalactic radio sources over the whole observable range of overall sizes; (2) detailed studies of the jet parameters at the working surfaces between the jets and the external medium (the hot spots) in CSOs; and (3) use of the number–overall size counts to determine, empirically, the evolution of luminosity with size in these objects. The eventual aim is a physical theory which predicts the evolution in size and luminosity of these objects, from the creation of the jet in a young active galaxy, to the expiration of the large-scale jet. The determination of empirical relationships which describe the evolution could play a vital role in the development of such a physical theory.

2.2. *An Empirical Approach to Evolution*

A comprehensive theory of the evolution of powerful extragalactic radio sources must include the evolution of both their luminosity and size with time. These observables depend upon the jet physics and the properties of the external medium. The relationship between the radio luminosity and the properties of the jet and external medium is complex, but, if the jet is confined by ram pressure with the external medium, then the instantaneous velocity of advance of the jet, v_a, is related to the pressure in the hot spot, p, and the density in the external medium, $\rho_{\rm ext}$, by the simple ram pressure relation

$$p = \rho_{\rm ext} v_a^2 \ . \tag{1}$$

The pressure in the hot spot is significantly greater than that in the lobe, so that from equation (1) it might be expected that the hot-spot advance speed exceeds that of the lobe. However, it is clear from the observations that the average speed of advance of the lobe must equal the average speed of advance of the jet; otherwise hot spots would protrude well in front of the lobes, which is never observed. One possible explanation is that changes in jet direction cause the jet to begin drilling out the lobe cavity from farther back, and that the instantaneous advance speed of the jet is actually much higher than the average jet advance speed (Scheuer 1982). Other possibilities are that the jet may be deflected at the hot spot (e.g., Lonsdale & Barthel 1984; Norman 1993), and hence drill out a much broader cavity while advancing steadily at the speed given by equation (1) for the jet; or that, while the advance speed of the hot spot is set by momentum conservation (eq. [1]), the energetic particles deposited by the jet in the vicinity of the hot spot drive a sideways expansion of the lobe at speed $v_a(p_l/p)^{1/2}$, where p_l is the pressure in the lobe. We show in § 4.1 that the observations support the latter interpretations, i.e., it appears that in powerful extragalactic radio sources the speed of advance of the lobes is not very different from the instantaneous speed of advance of the hot spot.

It might be thought that the advance speed is set by the pressure in the lobes rather than the pressure in the hot spots. This cannot be the case, however, since it would produce spherical radio sources rather than the elongated sources which we observe. Furthermore, as shown in § 4.1, in the case of Cygnus A we find that the advance speed of the lobe is equal to the advance speed of the hot spot. Nevertheless, we point out that it is easy to generalize the approach we adopt here to a model in which the lobe advance speed is a function of the hot-spot advance speed (see, e.g., Begelman 1995).

The ram pressure relationship of equation (1) enables us to determine the velocity of advance if the hot-spot pressure and the external density are known. However, in order to understand the evolution of an object, we must determine how the velocity of advance and pressure depend on external conditions and the thrust of the jet over the active lifetime of the source, i.e., we need to determine the function f,

$$v_a = f(F, \rho_{\rm ext}, T_{\rm ext}) \ , \tag{2}$$

where $T_{\rm ext}$ is the temperature of the external medium, and F, the thrust of the jet, is given by

$$F = \pi r^2 p \ , \tag{3}$$

where r is the radius of the hot spot. Provided that any entrainment of the surrounding medium is small, the thrust

of the jet delivered to the hot spot is determined by the central engine, independent of conditions in the external medium in the vicinity of the observed jets. The determination of the function f is the most basic step to be taken in understanding the evolution of powerful extragalactic radio sources, since not only would it enable us to determine the evolution in size of these objects, but, through use of the number–overall size counts, it would also reveal the luminosity evolution.

It might, at first sight, appear from equation (1) that over the lifetime of a jet v_a must have an explicit dependence upon $\rho_{\rm ext}$. However, this is not so because it is possible that, as a jet advances through a medium of varying density or temperature, the hot-spot pressure and size "self-adjust" in such a way as to maintain a constant advance speed. Simulations by Lind et al. (1989) suggest that the terminal speed of advance of a relativistic jet is set by the sound speed in the external medium, which depends upon the temperature of the external medium but not the density (see Paper II).

Note that even if the terminal velocity of the jet were set by the sound speed in the external medium, an implicit dependence of v_a on $\rho_{\rm ext}$ can be introduced through the temperature and pressure of the external medium. It is clearly important to determine from observations, if possible, how v_a depends on $\rho_{\rm ext}$.

2.3. *Possible Forms of Evolution*

In order to clarify our discussion we, in concert with Fanti et al. (1995), classify double-lobed extragalactic radio sources according to their overall physical size as follows: We define compact symmetric objects (CSOs) as those objects with lobe separations of less than 1 kpc, medium-sized symmetric objects (MSOs) as those objects with lobe separations between 1 kpc and 15 kpc, and large symmetric objects (LSOs) as those objects with lobe separations greater than 15 kpc.

We propose a unifying hypothesis in which CSOs evolve into MSOs, which, in turn, evolve into LSOs. A similar evolutionary sequence was first proposed by Readhead & Hewish (1976), which they illustrated with objects of increasing overall size, 3C 147 → 3C 295 → 3C 9 → 3C 215. The separations of the lobes in these four objects are 1.5, 16, 98, and 237 kpc. The quasar 3C 147 is morphologically very similar to the five PR CSOs, all of which have a bright jet on one side of the center of activity and a more diffuse lobe on the other side. The similarity to 0404+768 is particularly striking. On our classification scheme 3C 147 is a small MSO, the radio galaxy 3C 295 is a small LSO, close to the MSO:LSO border, and the objects 3C 9 and 3C 215 are both LSOs. The evolutionary sequence which we are proposing, in which the sequence of Readhead & Hewish is extended down to the smallest CSOs, was first suggested by Hodges & Mutel (1987). Fanti et al. (1995) have also proposed this sequence.

Under the assumption of this unifying hypothesis it is possible to draw some general conclusions concerning the evolution of powerful extragalactic radio souces, independent of details of the particular evolutionary model.

Readhead (1995) has discussed three possible forms of evolution: pure luminosity evolution (i.e., constant velocity), pure velocity evolution (i.e., constant luminosity), and combined luminosity and velocity evolution. He showed that the limits on the density of the external medium derived in Paper II rule out pure velocity evolution. Significant luminosity evolution is required to explain these objects under our unifying hypothesis (see also Fanti et al. 1995 on this point). We do not repeat those arguments here, but we focus on one particular aspect of the discussion, viz., the dependence of the hot-spot pressure on the external density.

3. CSOs AS A LABORATORY FOR JET PHYSICS

We now assume as a working hypothesis that the function $f(F, \rho_{\rm ext}, T_{\rm ext})$ of equation (2) may be written in the form

$$v_a = \kappa_v \rho_{\rm ext}^{-m} , \tag{4}$$

where κ_v may depend upon the thrust of the jet. We also assume that the hot spots that we have observed in 0108+388, 0710+439, and 2352+495 are fairly stable features in these jets, and that the pressure differences that we see between the two hot spots in all three objects are not transient. We note that, in all three objects, the higher pressure hot spot is on the side of the brighter jet (see Fig. 1 of Paper II). We suggest that both the higher brightness of this jet and the higher pressure of the hot spot are due to higher external density on this side of the object.

It is clearly important to consider whether we have missed any CSOs, and thus introduced a selection effect in choosing these three objects. This point is discussed in § 2.3 of Paper II, where we show that there is not a selection bias; it is clear from our study of the complete PR sample that no galaxies with overall sizes less than 1 kpc have been missed from the CSO class owing to observational surface brightness limitations.

3.1. *The Ram Pressure Confinement of Two Oppositely Directed Jets*

Consider a jet of constant thrust F, moving through a medium of density $\rho_{\rm ext}$, which is a power-law function of the distance R from the origin of the jet, i.e.,

$$\rho_{\rm ext}(R) = \kappa_\rho R^{-n} . \tag{5}$$

We assume that the advance speed of the jet is given by equation (4). Thus $v_a(R) = \kappa_v \kappa_\rho^{-m} R^{nm}$.

The age of the jet when it reaches the observed distance, R_o, from the origin is simply given by $\tau_j = \int_0^{R_0} v_a^{-1}\, dR$. Thus, provided $n < 1/|m|$, we have

$$\tau_j = \left(\frac{1}{1-nm}\right)\kappa_\rho^m \kappa_v^{-1} R_o^{1-nm} . \tag{6}$$

We will show below that the observations of CSOs indicate that $m \sim 0$, so that the allowed range of n on this analysis extends up to $n \gg 1$.

We assume that the thrusts of the two oppositely directed jets in a particular CSO are equal. This will be justified later. For two jets of equal thrust and age, equation (6) yields

$$\frac{\kappa_{\rho 1}}{\kappa_{\rho 2}} = \left(\frac{R_{o1}}{R_{o2}}\right)^{(nm-1)/m} , \tag{7}$$

where the subscripts 1 and 2 refer to the two oppositely directed jets. Equations (5) and (7) show that

$$\frac{\rho_{\rm ext}(R_{o1})}{\rho_{\rm ext}(R_{o2})} = \left(\frac{R_{o1}}{R_{o2}}\right)^{-1/m} . \tag{8}$$

From equations (1), (4), and (8), we have

$$\frac{p_{o1}}{p_{o2}} = \left(\frac{R_{o1}}{R_{o2}}\right)^{2-1/m}, \quad (9)$$

and from equations (4), (5), and (7) we find

$$\frac{v_a(R_{o1})}{v_a(R_{o2})} = \left(\frac{R_{o1}}{R_{o2}}\right). \quad (10)$$

Thus the ratio of the velocities of the two hot spots at a particular epoch is simply given by the ratio of their distances from the core, just as in the case of an external medium with constant (but different) densities on the two sides, and is independent of n. We see from equations (3) and (9) that

$$\frac{r(R_{o1})}{r(R_{o2})} = \left(\frac{R_{o1}}{R_{o2}}\right)^{(1-2m)/2m}. \quad (11)$$

Thus m can be determined from the ratio of the hot-spot sizes and the ratio of their distances from the core. Furthermore, combining equations (8) and (11), we have

$$\frac{r(R_{o1})}{r(R_{o2})} = \left[\frac{\rho_{\rm ext}(R_{o1})}{\rho_{\rm ext}(R_{o2})}\right]^{m-1/2}. \quad (12)$$

Note that equations (7)–(12) all refer to *ratios* between parameters in the two oppositely directed jets at the same instant. They do not, for example, tell us how the parameters themselves vary with R. We use these ratios below to determine m. Once we have done this, we may use this value of m to determine the behavior of a single jet as a function of the external density, since the following relationships are implied by equations (3) and (4):

$$p = \kappa_v^2 \rho_{\rm ext}^{1-2m}, \quad (13a)$$

$$r = (F/\pi)^{1/2} \kappa_v^{-1} \rho_{\rm ext}^{m-1/2}. \quad (13b)$$

Furthermore, in the case of equipartition, the flux density of the hot spot, S, is proportional to $r^3 p^{7/4}$, i.e.,

$$S \propto \kappa_v^{1/2} (F/\pi)^{3/2} \rho_{\rm ext}^{1/4-m/2}. \quad (13c)$$

Application of equation (5) shows how these parameters vary with R on our model.

3.2. *Comparison with Observations*

We are now in a position to compare the behavior expected in two oppositely directed jets with that observed in CSOs. In our VLBI survey of objects in the PR sample (Paper II), we found three CSOs (0108+388, 0710+439, and 2353+495) in which hot spots were detected in both lobes. In all three objects the two hot spots are almost equidistant from the center of activity, provided that we have identified this correctly (Taylor et al. 1996).

In Paper II we determined the physical properties of the hot spots in 2352+495. We have carried out the same calculations for 0108+388 and 0710+439. The relevant parameters are given in Table 1, and in Figure 1 we show the minimum hot-spot pressures in these objects, and the distance R of the hot spot from the center of activity. We have calculated the jet power and thrust, as described in Paper II, and these results are also given in Table 1. We assume throughout that the uncertainties in the observed hot-spot size, flux density, and distance from the core are 10%, 10%, and 5%, respectively, except that, in the case of 0108+388, we assume a 10% uncertainty in the distance of the hot spot from the core. Note that $F \propto S^{4/7}\theta^{2/7}$, where S and θ are the hot-spot flux density and angular size, so that, given these uncertainties, F is a well-determined quantity. We see that the results on 0108+388 and 0710+439 are very similar to those derived for 2352+495 in Paper II. In all three cases the thrusts of the two oppositely directed jets are very similar.

We therefore assume equal thrusts for the two oppositely directed jets in each of our three CSOs, and we attribute the observed differences in the pressure, size, and distance of the hot spots on either side of the nucleus primarily to differences in the external medium. It is possible that the hot spots are transient features, and that the pressure and size of the hot spots vary as the source advances, alternately building up a large, lower pressure hot spot and then sloughing it off to one side and starting again with a smaller, higher pressure hot spot (Lind et al. 1989; Clarke 1993). While this is certainly possible, it seems likely that the hot spots are reasonably permanent features in CSOs, because in all three of our prime CSO candidates the higher pressure hot spot is on the same side of the center of activity as the brighter jet, and we believe that both the higher pressure hot spot and the brighter jet are caused by higher external pressure. However, this remains a crucial part of the theory to be tested. We will assume for the present discussion that the hot spots are fairly long-term features, and that the differences in observed pressures in the hot spots reflect differences in the average hot-spot pressures on the two sides of the center of activity.

For each CSO we have an internal normalization for the jet power and thrust, and the ratios of the observed pressures and sizes of the hot spots must depend almost entirely on the ratios of the external densities. We now proceed on this assumption, and we show that if these three objects are indeed confined by the ram pressure interaction with the external medium, the thrust of the jets remains constant as

TABLE 1

PHYSICAL CHARACTERISTICS OF THE HOT SPOTS

Object (Component)	Distance (pc)	Diameter (pc)	Opening Angle	Pressure (dyne cm^{-2})	Thrust (dyne)	Thrust Ratio	Error
0108+388 (N).....	13.5	2.50	16	1.4×10^{-4}	5.9×10^{33}	1.4	±0.1
0108+388 (S)	9.8	4.50	17	2.9×10^{-5}	4.2×10^{33}		
0710+439 (N).....	44.4	3.70	7	6.4×10^{-5}	6.1×10^{33}	1.6	±0.15
0710+439 (S)	45.1	6.40	6	1.3×10^{-5}	3.7×10^{33}		
2352+495 (N).....	57.4	2.69	4	1.9×10^{-5}	9.2×10^{32}	1.1	±0.1
2352+495 (S)	60.0	6.36	5	3.1×10^{-6}	8.2×10^{32}		

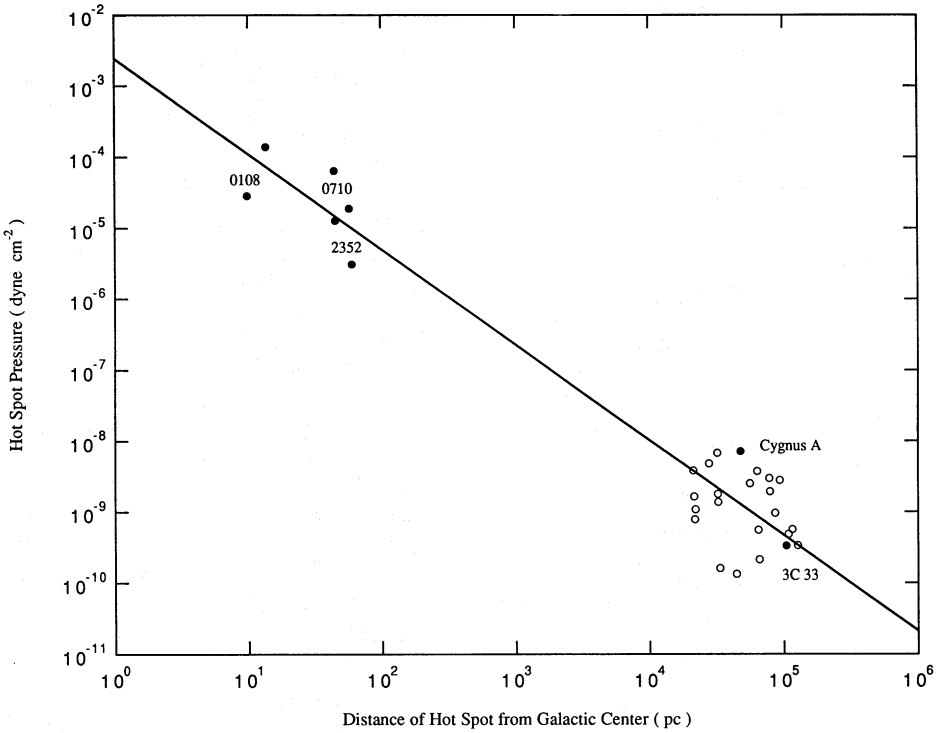

FIG. 1.—Hot-spot pressures and distances. The pressures and distances from the nucleus are shown here for the hot spots in 0108+388, 0710+439, 2352+495, Cygnus A, and 3C 33 (*filled circles*); and the quasars in the Bridle et al. (1994) sample (*open circles*). The line shows the best fit, $p \propto R^{-1.3}$ (see text).

they advance—independent of the properties of the external medium—as one would expect, since the thrust of the jet must be set by the central engine.

We begin by assuming that the hot-spot pressure and size are related by $p \propto r^a$. Hence, from the ratio of the hot-spot pressures on the two sides, and the ratio of the hot-spot sizes, we find an average value for a from the three CSOs of $a = -2.4 \pm 0.4$ (see Table 2). This is consistent with the value expected for a jet whose thrust is independent of external conditions, i.e., $a = -2$. We therefore assume for the remainder of the analysis that $a = -2$.

Note that our assumption of equipartition means that we have set $p \propto S^{4/7} r^{-12/7}$. If there were no dependence of p upon S, then we would expect a to be close to -2. However, one only has to change S appreciably in order to destroy the relationship. Thus the good agreement obtained between the observed and expected values of a, which depends on the value of S, gives confidence that these objects are confined by ram pressure and that any relativistic beaming effects in the hot spots are small. Note that the estimated thrust ratios of the two jets in all three objects agree to within a factor ~ 1.5 (see Table 1), although they appear to differ slightly, but significantly, from unity in 0108+388 and 0710+439. We assume this is because of mild relativistic beaming, and we have therefore applied a relativistic beaming correction to the flux densities in all three CSOs so as to equalize the thrusts of the two jets in each object.

We now determine the dependence of hot-spot advance speed on the external density using the relations given in equations (9) and (11). The results are shown in Table 2. The average value for the three CSOs is $m = 0.00 \pm 0.02$ (see Table 2). Application of equations (13a) and (13b) yields $p \propto \rho_{\rm ext}^{1.00 \pm 0.04}$ and $r \propto \rho_{\rm ext}^{-0.50 \pm 0.02}$.

With the above value of m, the three relationships expressed by equations (13a)–(13c) show just how a relativistic jet confined by ram pressure adjusts the pressure, size, and flux density of the hotspot to the external density. We see that the velocity is independent of the external pressure, so that if CSOs evolve into LSOs, this must be pure luminosity evolution.

Setting $a = 2$ and $m = 0$, so that

$$v_a = \kappa_v \,, \tag{14}$$

we see that the observations are consistent with the follow-

TABLE 2

DERIVED POWER-LAW INDICES FOR JET PARAMETERS

Assumed or Derived Form of Relationship	Power-Law Index	0108+388	0710+439	2352+495	Weighted Mean
$p \propto r^a$	a	-2.6 ± 0.7	-2.9 ± 0.9	-2.1 ± 0.5	-2.4 ± 0.4
$v_a \propto \rho_{\rm ext}^{-m}$:					
From pressure (eq. [9])[a]	m	-0.3 ± 0.2	0.01 ± 0.04	0.02 ± 0.04	0.01 ± 0.02
From size (eq. [11])[a]	m	-0.2 ± 0.1	0.01 ± 0.07	0.03 ± 0.04	-0.01 ± 0.02
From pressure (eq. [9])[b]	m	-0.5 ± 0.3	0.01 ± 0.06	0.02 ± 0.04	0.01 ± 0.02

[a] Using uncorrected flux densities (see text).
[b] Using flux densities corrected for relativistic beaming to equalize the jet thrusts (see text).

ing relationships from equation (13):

$$p = \kappa_v^2 \rho_{\rm ext} , \tag{15a}$$

$$r = (F/\pi)^{1/2} \kappa_v^{-1} \rho_{\rm ext}^{-1/2} , \tag{15b}$$

and

$$S \propto \kappa_v^{1/2} (F/\pi)^{3/2} \rho_{\rm ext}^{1/4} . \tag{15c}$$

We have, as yet, no independent estimates of the external densities in these three objects, so we cannot determine the dependence of κ_v on F. We will assume that κ_v is independent of F, i.e., that it is the same for all sources. This is an important part of the model which remains to be determined.

4. COMPARISON WITH LARGE-SCALE JETS

We now apply the simple relationships derived above to large-scale jets. In the above discussion we identified the hot spots of the CSOs with the working surfaces of the jets. We propose that these are to be compared with the *primary* hot spots observed in larger scale jets. Many of the hot spots reported in the literature have proved, with the advent of higher resolution observations, to be complex emission regions, now thought to be secondary hot spots (Carilli, Dreher, & Perley 1989b). Only very high resolution observations are adequate to determine the properties of the primary hot spots. The best example is provided by the observations of Cygnus A by Carilli et al. (1989a), which have comparatively high linear resolution because of the low redshift $z = 0.0561$. Here we can be confident that the primary hot spot has been resolved. In the highest resolution Cygnus A maps made by C. L. Carilli (1995, private communication) the resolution is a factor of 20 better than in the observations of Hargrave & Ryle (1974), yet the size of the primary hot spot is found to be only a factor of 3 smaller. We have taken a number of profile cuts across the primary hot spot on the 0".11 resolution map made by Carilli (1995, private communication), and hence determined the hot-spot size. Another feature which gives us confidence in identifying this as the working surface in Cygnus A is the clear evidence of a bow shock in front of this hot spot, as seen in rotation measure measurements by Carilli et al. (1989b). The pressure of the primary hot spot in Cygnus A, which we calculate from Carilli's 0".11 resolution map, is shown in Figure 1.

We note that if radio sources were "self-similar," i.e., if the CSOs were morphologically identical to Cygnus A but a factor of 10^3 smaller, the hot spots in CSOs would be approximately 10 times smaller than the components we have identified as hot spots, and higher resolution VLBI observations would be needed to resolve them. We are confident that this is not the case, because we have higher resolution observations of these objects which reveal that the hot spots are indeed resolved and confirm the sizes that we have assumed here. We are therefore confident that the hot spots we have observed in CSOs are the correct counterparts to be compared with the primary hot spot in Cygnus A.

We are now in a position to determine the relationships between hot-spot pressure, etc., and external density for large-scale jets. The value of the external density at the position of the primary hot spot in Cygnus A is 0.01 cm^{-3} (Arnaud et al. 1984; Harris et al. 1994). We assume $m = 0$, and hence, applying equation (15a) to the primary hot spot in Cygnus A, we derive $\kappa_v = 0.022c$.

4.1. *Hot Spot and Lobe Advance Speed*

We now discuss the relationship between the instantaneous hot-spot advance speed and the speed of advance of the lobes.

As we have seen, the velocity of advance of the primary hot spot in Cygnus A, derived from the observed external density and hot-spot pressure, is $0.022c$. This value is comparable to the advance speeds of the lobes that are often assumed for LSOs.

We now derive the advance speed of the western lobe in Cygnus A. We have determined the pressure in the external medium of Cygnus A, at the position of greatest width of the lobe, from the X-ray results of Arnaud et al. (1984) to be 1.1×10^{-10} dynes cm^{-2}. We calculate the minimum pressure of the lobe to be over 8×10^{-10} dynes cm^{-2}, i.e., almost an order of magnitude greater than the external pressure. We are confident that the external pressure has not been underestimated, nor the lobe pressure overestimated, by more than about 50%, and therefore that the external pressure does not balance the lobe pressure. We assume, therefore, that the lobe pressure is balanced by ram pressure with the external medium, because of the sideways expansion of the lobe. A detailed discussion of the lobe and external pressure in Cygnus A is given by Begelman & Cioffi (1989), who drew the same conclusion. The sideways expansion speed is then $7 \times 10^{-3}c$, and we may determine the lobe advance speed from this speed and the ratio of the width of the lobe to the distance of the front surface of the lobe from the core. The ratio of the half-width to jet length is 3.8 ± 0.5, so that the lobe advance speed is $0.024c \pm 0.003c$. This is equal, to within the errors, to the instantaneous hot-spot advance speed. Thus, in the object for which we have the best observations of the primary hot spot, it appears that the instantaneous advance speed of the hot spot is not appreciably different from that of the lobe. We point out, however, that small differences, of up to about a factor of 2, between these two speeds would not greatly alter our interpretation. Based on the above derived velocities for the primary hot spot and the western lobe in Cygnus A, we therefore assume that $v_a = 0.02c \pm 0.01c$ in Cygnus A.

The general belief that the hot spots are advancing instantaneously at greater speed than the lobes is based on the observation that the hot spots are "overpressured" relative to the lobes. It is therefore important to consider whether the pressure in the primary hot spot of Cygnus A is unusually low. Unfortunately, as already mentioned, there are few high-luminosity objects as close as Cygnus A, and the Cygnus A map provides the highest available linear resolution observation of any powerful extragalactic radio source. However, the recent work by Bridle et al. (1994) on 3CR quasars provides a suitable comparison sample. The hot-spot size in Cygnus A is about 300 pc. The jet thrusts in the 3CR quasars studied by Bridle et al. (1994) are, on average, a factor of 17.6 greater than the thrust in the Cygnus A jet. Furthermore, the density of the Cygnus A cluster is unusually high, and the external density for a typical object might well be 30 times lower than that for Cygnus A. The relationship given by equation (15b) then implies a size for these hot spots of ~ 5 kpc, or an angular size $\sim 1''$—well above the 0".35 resolution of the obser-

vations of Bridle et al. It therefore seems likely that the hot spots have been resolved in the observations of Bridle et al., and that they provide a reliable estimate of the pressures of the hot spots.

We have calculated the hot-spot pressures for the objects in the sample of Bridle et al., using the same assumptions as for the CSOs (see Paper II). The pressures that we calculate are typically a factor of ~ 6 lower than those calculated by Bridle et al. This difference is explained by a factor of 2, due to our assumption of an electron-positron plasma, and by a factor of $(1.8)^{12/7}$, due to the correction by a factor of 1.8 of the fitted Gaussian model to approximate a spherical source brightness distribution (see Paper II). Our calculated pressures are shown in Figure 1. We see that there is no evidence that the pressure determined for the Cygnus A primary hot spot is too low; it is near the top of the distribution, as we would expect on account of the high density of the external medium. We suggest, therefore, that the result that we have found for Cygnus A is not unusual, and that the instantaneous speed of advance of the hot spots in powerful extragalactic radio sources is the same, to within a factor of ~ 2, as the lobe advance speed.

5. THE DENSITY OF THE EXTERNAL MEDIUM

We are now in a position to determine both the variation of density of the external medium with R and the density of the external medium in CSOs.

From the data shown in Figure 1 we find that $p \propto R^{-1.3 \pm 0.13}$, where the error is based upon the observational errors given in the previous section. We combine this result with that of equation (15a), and hence, through the application of equation (5), we determine that $n = 1.3 \pm 0.13$. We use the relationships expressed by equations (15), and the value of κ_v derived above. We assume a density of $n_p = 3.3 \times 10^{-4}$ cm^{-3} at 100 kpc, which is a typical external density in LSOs at this distance. The corresponding hot-spot pressures on this model are shown by the line in Figure 1.

The density of the external medium around CSOs implied by this model is ~ 3 cm^{-3} at 100 pc from the center of activity, in good agreement with the value derived for the external medium in the narrow-line region (see Paper II), and consistent with the observational constraints on the densities of H II, H I, and H_2 found in Paper II. Therefore, the relationships that we have derived for the dependences of the hot-spot parameters on external density for the CSOs and for Cygnus A demand modest external densities for the CSOs, and are consistent with the *Fast* model (advance speed $\sim 0.02c$) discussed in Paper II.

6. THE EVOLUTION OF EXTRAGALACTIC RADIO SOURCES

If the density law expressed by equation (5) is indeed applicable over the whole range of sizes, then, in principle, we now have an empirical set of relationships which fully describe the evolution in size of powerful extragalactic radio sources. This, in conjunction with the observed number–flux density counts, enables us to place stringent constraints on the luminosity evolution.

We are, therefore, in a position to discuss the evolution of powerful extragalactic radio sources. We assume that the *Fast* model is correct (i.e., sources expand with constant speed $v_a \approx 0.02c$), and consider the unified model for the evolution of these objects in which we assume that CSOs evolve first into MSOs, and finally into LSOs. We recognize that this is probably not the only evolutionary path for powerful extragalactic radio sources, but we suggest that it is the *primary* path. Some objects may exhaust their fuel before the jets have emerged from the galaxy, others may be slowed by entrainment and turn into Fanaroff-Riley type objects. However, the general picture seems clear, and these other paths are interesting, but minor, variations.

6.1. *The P-D Diagram and Sample Statistics*

In order to investigate the implications of the relationships that we have derived for the evolution of powerful extragalactic radio sources, we consider the complete sample of Laing, Riley, & Longair (1983, hereafter LRL). To minimize the effects of cosmological evolution, we consider only objects in the range $0.2 \leq z \leq 1$, the minimum redshift range of objects in this sample which can be studied with reasonable statistics.

Only 13% of objects in the LRL subsample have sizes in the MSO range (1–15 kpc). This is smaller than the expected fraction of 20% MSOs (Fanti et al. 1995). The shortfall is caused by objects missed in the LRL sample because of its low selection frequency (178 MHz), which misses a significant number of MSOs because of synchrotron self-absorption. Fanti et al. (1995) determined this fraction from a comparison of low-frequency and high-frequency surveys; thus this fraction is well determined from the observations. We divide the objects into seven equal bins in log R, of width $\Delta \log R = 0.5$. In order to correct for the six sources missed because of synchrotron self-absorption, which we estimate from the Fanti et al. result, we have increased the number of objects in the three bins with an overall size less than 15 kpc by a total of six objects, by adding one object to the smallest bin and five objects to the third bin. We chose this distribution because it yielded the smoothest N versus log R curve. Note that this is an exploratory step; we are trying to find whether it is possible to make a model which is consistent with all of the observations. In Figure 2 we show the resulting distribution of objects. We have fitted power laws of different slopes to the first five data points. We ignore the data for the largest objects (≥ 158 kpc), because it is clear that effects of the upper cutoff in size and age of these objects is affecting these numbers. Note that since we have chosen the distribution of the six missing objects in the first three bins to give the smoothest line in Figure 2, our confidence limits should be regarded as exemplary rather than rigorous. However, almost all random redistributions of these six objects within the first three bins would have placed the points between the dashed lines, so we do not believe that our procedure is misleading. We set $N(\log R) \propto R^w$, and we find that $w_{\rm LRL} = 0.47^{+0.38}_{-0.25}$, where the upper and lower limits denote the 95% confidence limits in χ^2 for three degrees of freedom, since we have fitted a mean and a slope to five points. Our assumption that N varies as a power law with log R implies that the total source flux density depends on an overall size as $S \propto R^q$, in which case, since the integral number–flux density counts at these flux density levels have slope $-3/2$, we have $q = \frac{2}{3}(nm + w - 1)$. The 95% confidence limits on w then yield $q_{\rm LRL} = -0.35^{+0.25}_{-0.17}$ for $m = 0$.

We compare this result with the observed luminosities of the objects in Figure 3. Here we have indicated the expected variation of luminosity with overall size, $P \propto R^q$, for $q = -0.35$, $q = -0.10$, and $q = -0.52$ (corresponding to

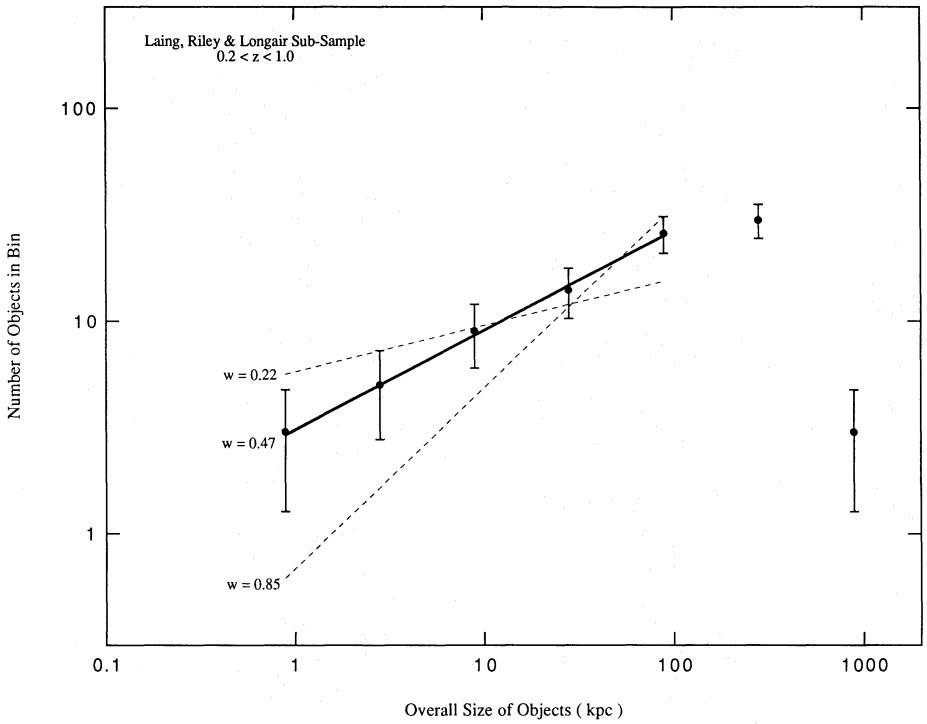

FIG. 2.—Number vs. overall size relation. The numbers of objects, from the subsample of the Laing, Riley, & Longair (1983) sample with $0.2 < z < 1.0$, in intervals $\Delta(\log R) = 0.5$. Six objects have been added to the first three bins to correct for objects missed due to synchrotron self-absorption (see text). The solid line is the minimum χ^2 fit to the data in the lower five bins, and the two dashed lines are the 95% confidence lines.

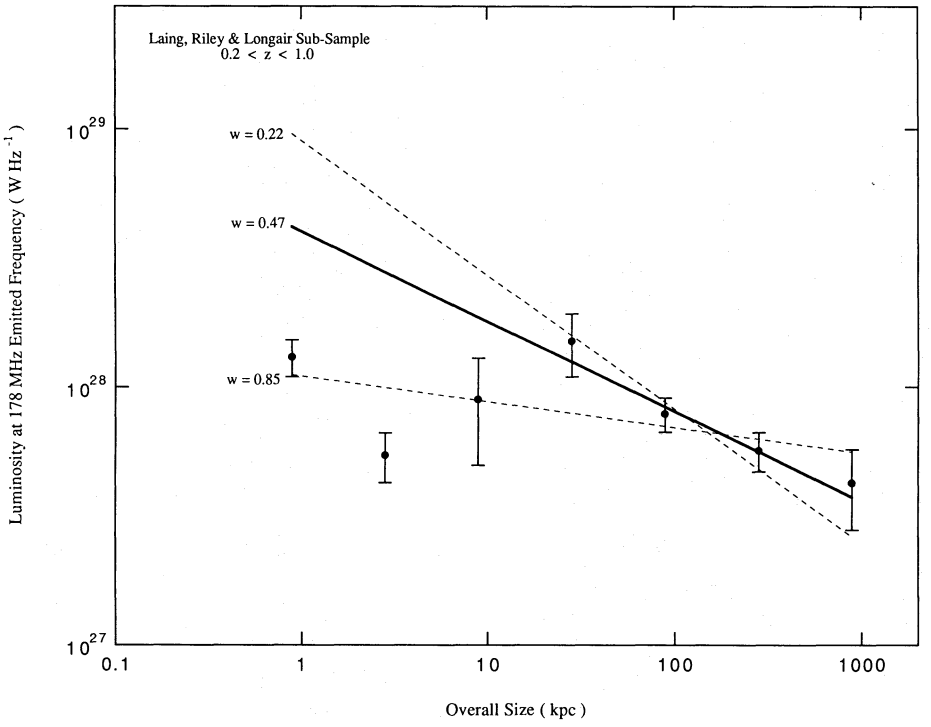

FIG. 3.—Luminosity vs. overall size relation. The luminosities of the objects in the subsample of the Laing, Riley, & Longair sample with $0.2 < z < 1.0$. The lines corresponding to the three values of w from Fig. 2 are shown. The minimum χ^2 fit to the data from the top four bins is indistinguishable from the $w = 0.47$ ($q = -0.35$) line. The poor fit for overall sizes less than 30 kpc is likely due to high-luminosity objects which have been missed at 178 MHz—the selection frequency of the LRL sample—because of synchrotron self-absorption (see text).

$w = 0.47$, $w = 0.85$, and $w = 0.22$). We see that the derived luminosity variation fits the observations well for objects larger than 30 kpc; the line marked $w = 0.47$ is indistinguishable from the least-squares fit to the top four data points. The observed drop-off in luminosity below 30 kpc is expected on this model, since the six objects which have dropped out of the sample due to synchrotron self-absorption, and which we added to the number counts of Figure 2, will be the highest luminosity objects in the smaller bins. Therefore we know that the mean luminosities of the objects in these bins, after correcting for objects lost because of synchrotron self-absorption, lie above the mean luminosities plotted in Figure 3. There is some danger in fitting the luminosities to the upper two bins, in which the numbers are dropping because of sources dying out. However, very few, if any, dying LSOs are known. Thus it appears that these objects fade rapidly once the supply from the central engine ceases. We are therefore assuming that the luminosities are not diluted by dying objects.

We see that our model provides a good fit to all the observations. The best-fit result for q implies a factor of 8 decrease in luminosity as the source expands from 500 pc to 200 kpc in overall size, while the lower limit is almost consistent with no luminosity evolution, and the upper limit implies a factor of 13 decrease in luminosity over this range. It therefore appears that, on our unifying hypothesis, powerful extragalactic radio sources undergo a considerable decrease in luminosity as they expand from 500 pc to 200 kpc. We note that Fanti et al. (1995) also concluded that MSOs must decrease in luminosity if they evolve into LSOs.

From the numbers of objects in our complete high-frequency samples we estimate that the fraction of objects which are CSOs is $10\% \pm 5\%$ (95% confidence) (Paper II). Fanti et al. (1995) have shown that $20\% \pm 5\%$ (95% confidence) of objects in a carefully selected sample are MSOs (where the uncertainty is our own estimate from the statistics). Therefore the ratio of MSOs to CSOs in a carefully selected sample (in which due allowance has been made for the loss of sources in low-frequency samples due to synchrotron self-absorption) is 2.0 ± 1.1 (95% confidence). This yields a value of $w_{\mathrm{CSO:MSO}} = 0.32^{+0.13}_{-0.24}$, and hence a power-law dependence for the luminosity evolution between the CSO and MSO phases of $q_{\mathrm{CSO:MSO}} = -0.45^{+0.12}_{-0.16}$ (95% confidence). Note that the derived ranges for q_{LRL} and $q_{\mathrm{CSO:MSO}}$ overlap, so that the luminosity evolution in the phases CSO—MSO—LSO, i.e., from 10 pc to 150 kpc, can be described by a single–power-law luminosity evolution. For a value of $q = -0.35$, for example, the luminosity would decrease by a factor of 30 over this range.

The derived value for q indicates the variation of lobe flux density with R, since it is the lobes that dominate the radio emission. The variation of the hot-spot flux density with R on our model determined from equation (15c) and our derived dependence of $\rho_{\mathrm{ext}} \propto R^{-1.3}$, is $S \propto R^{-0.33}$. Thus the variation with R of the flux densities of the lobes and of the hot spots are very similar, and we would expect the relative strengths of the hot spots and lobes to remain approximately constant as a source expands. This is consistent with the observations of hot spots and lobes in CSOs, MSOs, and LSOs.

We see, therefore, that both CSOs and MSOs undergo significant luminosity evolution on this model. In Paper II we pointed out that CSOs have an unusually high ratio of radio luminosity to jet power, and that the typical ratio of the flux density in the jets, hot spots, and lobes to jet power is ~ 0.33. The reduction in source luminosity due to evolution on our model would bring this ratio down to levels which are in good agreement with the ratios observed in LSOs. We suggest that the change in luminosity in CSOs and MSOs is due to the decrease in the external density with distance from the core, which we have shown to vary according to $\rho_{\mathrm{ext}} \propto R^{-1.3}$.

There are a number of studies of the correlation of median size with luminosity of extragalactic radio sources (e.g., Oort et al. 1987; Singal 1988; Kapahi 1989; Nilsson et al. 1993; Neeser et al. 1995), and there is some uncertainty on whether the median size has a positive (Oort et al. 1987; Kapahi 1989), zero (Neeser et al. 1995), or negative (e.g., Nilsson et al. 1993) correlation with luminosity. The correlations over a wide range of luminosity classes are not to be confused with the evolution of individual objects—as has been pointed out by Oort et al. (1987). In fact, the magnitude of the correlation found by Oort et al. (1987) and Kapahi (1989), $R \propto P^{0.3}$, if applied to the evolution of a single object, would require $P \propto R^{3.3}$, and hence approximately constant emissivity (per unit volume) as the object expands, whereas it is clear that the emissivity decreases with increasing size of the emission regions because of declining magnetic field and particle energy densities.

7. CONCLUSIONS

The existing observational evidence is consistent with a "unified" interpretation of the major classes of powerful extragalactic radio sources, in which the CSOs evolve into MSOs, which evolve in turn into LSOs. This scenario provides a simple interpretation of the relative numbers of objects in these classes, and their ranges of pressure and jet power.

The detailed model developed in §§ 3–6 appears to have many advantages. Its successes are (1) the demonstration that the velocity of advance is independent of external density, (2) the determination of the external density in CSOs, (3) the simple interpretation of the high ratio of radio luminosity of the lobes and jet to the jet power in CSOs, and (4) the unification of CSOs MSOs, and LSOs into a single evolutionary sequence.

If our suggested luminosity evolution is correct, then the precursors of powerful objects, like Cygnus A, were considerably more luminous than the CSOs we observe, and the CSOs we have discussed in this paper will evolve into low-luminosity Fanaroff-Riley type II (FR II) objects. This luminosity evolution, if true, will greatly aid the study of the early stages of development of FR II objects, since otherwise highly luminous infant FR II objects will be exceedingly rare.

Compact symmetric objects are much younger than other classes of powerful extragalactic radio sources, therefore they provide an interesting view of active galaxies at a comparatively early stage after the activity has commenced. They also provide a unique probe of the interstellar medium within the central 100 pc of active galaxies. Both of these factors will likely prove of critical importance to our understanding of the generation and evolution of active galaxies.

We thank Mitch Begelman, Roger Blandford, Dave De Young, Mike Norman, and Sterl Phinney for useful dis-

cussions. We also thank the staffs of the observatories in the global VLBI network and of the VLBA for their vital contributions to this work. This work was supported by grants from the National Science Foundation (AST 88-14554, AST 91-17100, and AST-9420018). This work is based on data obtained with the VLBA of the NRAO, which is operated by Associated Universities, Inc., under cooperative agreement with the National Science Foundation.

REFERENCES

Arnaud, K. A., Fabian, A. C., Eales, S. A., Jones, C., & Forman, W. 1984, MNRAS, 211, 981
Baade, W., & Minkowski, R. 1954, ApJ, 119, 206
Baldwin, J. E. 1982, in Extragalactic Radio Sources, ed. D. S. Heeschen & C. M. Wade (Dordrecht: Reidel), 21
Begelman, M. C. 1995, in Cygnus A—a Study of a Radio Galaxy, ed. C. Carilli & D. E. Harris (Cambridge: Cambridge Univ. Press), in press
Begelman, M. C., & Cioffi, D. F. 1989, ApJ, 345, L21
Blandford, R. D. 1989, in Theory of Accretion Disks, ed. P. Meyer, W. Duschl, J. Frank, & E. Meyer-Hofmeister (Dordrecht: Kluwer), 35
———. 1993, in Astrophysical Jets, ed. D. Burgarella, M. Livio & C. P. O'Dea (Cambridge: Cambridge Univ. Press), 15
Blandford, R. D., & Rees, M. 1974, MNRAS, 169, 395
Bridle, A. H., Hough, D. H., Lonsdale, C. J., Burns, J. O., & Laing, R. A. 1994, A&A, 108, 766
Bridle, A. H., & Perley, R. A. 1984, ARA&A, 22, 319
Carilli, C. L. 1995, private communication
Carilli, C. L., Dreher, J. W., & Perley, R. A. 1989a, in Hotspots in Extragalactic Radio Sources, ed. K. Meisenheimer & H. J. Röser (Berlin: Springer), 51
Carilli, C. L., Perley, R. A., & Dreher, J. W. 1989b, ApJ, 334, L73
Carvalho, J. C. 1985, MNRAS, 215, 463
Clarke, D. A., Norman, M. L., & Burns, J. O. 1986, ApJ, 311, L63
Clarke, D. A. 1993, in Jets in Extragalactic Radio Sources, ed. K. Meisenheimer & H. J. Röser (Berlin: Springer), 243
De Young, D. S., & Axford, W. I. 1967, Nature, 216, 129
Fabian, A. C. 1995, in preparation
Fanti, C., Fanti, R., Dallacasa, D., Schilizzi, R. T., Spencer, R. E., & Stanghellini, C. 1995, A&A, 302, 317
Fanti, C., Fanti, R., Parma, P., Schilizzi, R. T., & van Breughel, W. J. M. 1985, A&A, 143, 292
Hargrave, P. J., & Ryle, M. 1974, MNRAS, 166, 305
Harris, D. E., Carilli, C. L., & Perley, R. A. 1994, Nature, 367, 713
Hodges, M. W., & Mutel, R. L. 1987, in Superluminal Radio Sources, ed. J. A. Zensus & T. J. Pearson (Cambridge: Cambridge Univ. Press), 168
Jennison, R. C., & Das Gupta, M. K. 1954, Nature, 172, 966
Kapahi, V. K. 1989, AJ, 97, 1
Kellermann, K. I., & Wall, J. V. 1987, in Observational Cosmology, ed. A. Hewett, G. Burbidge, & L. Z. Fang (Dordrecht: Reidel), 545
Kossl, D., Muller, E., & Hillebrandt, W. 1990a, A&A, 229, 378
———. 1990b, A&A, 229, 397
———. 1990c, A&A, 229, 401
Laing, R. A., Riley, J. M., & Longair, M. S. 1983, MNRAS, 204, 151 (LRL)
Leahy, J. P., & Williams, A. G. 1984, MNRAS, 210, 929
Lind, K. R., Payne, D. G., Meier, D. L., & Blandford, R. D. 1989, ApJ, 344, 89
Lonsdale, C. J., & Barthel, P. D. 1984, A&A, 303, 617
Neeser, M. J., Eales, S. A., Law-Green, J. D., Leahy, J. P., & Rawlings, S. 1995, ApJ, 451, 76
Nilsson, K., Valtonen, M. J., Kotilainen, J., & Jaakkola, T. 1993, ApJ, 413, 453
Norman, M. L. 1993, in Astrophysical Jets, ed. D. Burgarella, M. Livio & C. P. O'Dea (Cambridge: Cambridge Univ. Press), 211
Norman, M. L., Smarr, L., Winkler, K.-H. A., & Smith, M. D. 1982, A&A, 113, 285
Norman, M. L., Winkler, K.-H. A., & Smarr, L. 1983, in Astrophysical Jets, ed. A. Ferrari & A. G. Pacholczyk (Dordrecht: Reidel), 227
———. 1984, in NRAO Conf. Proc. 9, Physics of Energy Transport in Extragalactic Radio Sources, ed. A. Bridle & J. Eilek (Green Bank: NRAO), 150
Oort, M. J. A., Katgert, P., & Windhorst, R. A. 1987, Nature, 328, 500
Pearson, T. J., & Readhead, A. C. S. 1988, ApJ, 328, 114
Perley, R. A., Dreher, J. W., & Cowan, J. J. 1984, ApJ, 285, L35
Polatidis, A., Wilkinson, P. N., Xu, W., Readhead, A. C. S., Pearson, T. J., Taylor, G. B., & Vermeulen, R. C. 1995, ApJS, 98, 1
Readhead, A. C. S. 1995, Proc. Natl. Acad. Sci., 92, 11447
Readhead, A. C. S., Cohen, M. H., & Blandford, R. D. 1978, Nature, 272, 131
Readhead, A. C. S., & Hewish, A. 1976, MNRAS, 176, 571
Readhead, A. C. S., Taylor, G. B., Xu, W., Pearson, T. J., Wilkinson, P. N., & Polatidis, A. 1995, ApJ, 460 (Paper II)
Rees, M. 1971, Nature, 229, 312
Ryle, M., & Longair, M. S. 1967, MNRAS, 136, 123
Scheuer, P. A. G. 1974, MNRAS, 166, 513
———. 1982, in IAU Symp. 97, Extragalactic Radio Sources, ed. D. S. Heeschen & C. M. Wade (Dordrecht: Reidel), 163
Singal, A. K. 1988, MNRAS, 233, 87
Smarr, L., Norman, M. L., & Winkler, K.-H. A. 1984, Physica D, 12, 83
Taylor, G. B., Readhead, A. C. S., & Pearson, T. J. 1996, ApJ, in press
Thakkar, D. D., Xu, W., Readhead, A. C. S., Pearson, T. J., Taylor, G. B., Vermeulen, R. C., Wilkinson, P. N., & Polatidis, A. 1995, ApJS, 98, 33
Turland, B. D. 1975, MNRAS, 172, 181
Waggett, P. C., Warner, P. J., & Baldwin, J. E. 1977, MNRAS, 181, 465
Wilkinson, P. N., Polatidis, A., Readhead, A. C. S., Xu, W., & Pearson, T. J. 1994, ApJ, 432, L87 (Paper I)
Wilson, M. J., & Scheuer, P. A. G. 1983, MNRAS., 205, 449
Xu, W., Readhead, A. C. S., Pearson, T. J., Polatidis, A., & Wilkinson, P. N. 1995, ApJS, 99, 297